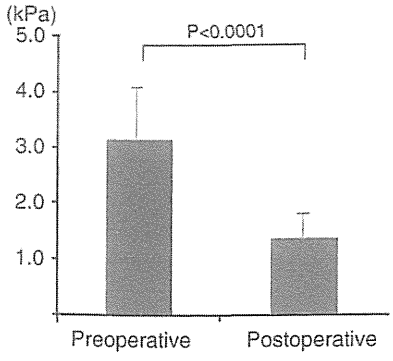

Fig. 25.6 The stress significantly reduced after surgery in the HIS group ($p<0.0001$)

The intramedullary stress of the HSI group significantly reduced after surgery. Reduction of the stress could be attributed to the restoration of spinal cord configuration obtained by surgical decompression. Consequently, reduction of the stress should involve in the decrease of the neuronal tissue damage and improvement of the neurological function.

25.7 Relationship of Intramedullary Stress to Sagittal Alignment of the Cervical Spine

Influence of the sagittal alignment of cervical spine on the postoperative change of intramedullary stress was investigated. The local kyphosis angle was measured on the lateral view of the radiograms. The local kyphosis angle was defined as the angle formed by two lines drawn along the posterior margin of the most cranial and caudal vertebral bodies forming the maximum local kyphosis according to the method described by Suda et al. [18]. Correlation between the local kyphosis angle and the reduction of the stress after surgery was calculated in HSI group. The HSI group were divided into two groups according to the local kyphosis angle: the lordosis group presenting the local kyphosis angle less than 0° (L group) and the kyphosis group presenting the local kyphosis angle exceeding 0° (K group).

The difference between preoperative and postoperative stress in the L group showed a high dispersion independently of the local kyphosis angle. The difference between the preoperative and postoperative stress was not correlated with the local kyphosis angle in the L group ($r=-0.45$, $p=0.07$). In the K group, two variables, however, were negatively correlated ($r=-0.59$, $p=0.02$) (Fig. 25.7). That is, as the kyphosis was severe, the reduction of the stress after surgery was decreased.

It was reported that the sagittal cervical alignment influences on the surgical outcome of CSM. Suda et al. reported that neurological recovery after expansive laminoplasty for CSM was poor in patients with the local kyphosis angle exceeding 13° [18]. Laminoplasty consists of two distinct mechanisms for decompression effect: a direct posterior decompression effect and an indirect anterior decompression effect. Indirect anterior decompression is considered to be attributed to the

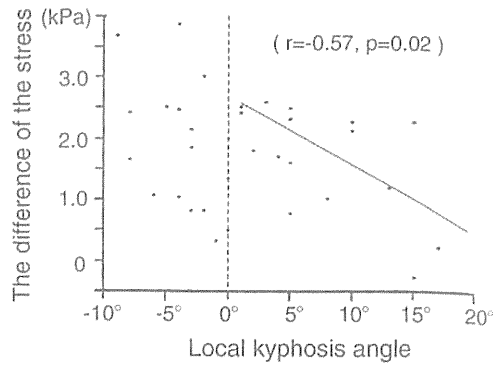

Fig. 25.7 Correlation between local kyphosis angle and the difference of the stress between before and after surgery in HIS group showing significantly negative correlation when the local kyphosis angle exceeded 0°

posterior spinal cord shifting from the anterior compressive lesions, which was demonstrated after posterior decompression surgery [19]. In cases with severe kyphosis, ventral compression after posterior decompression surgery is presumably likely to persist, resulting in poor surgical outcomes. In the present study, the deformity of the spinal cord remained after surgery in K group. It induced the less reduction of stress after surgery. The previous report that the severe kyphotic deformity is a risk factor for poor surgical outcomes was supported from a standpoint of intramedullary stress.

25.8 Conclusion

1. Intramedullary stress should be a highly important factor for the onset of CSM. When the intramedullary stress reaches at some extent, neurological dysfunction should become obvious.
2. Stress was found to be a more important prognosticator for the onset of CSM than the cross-sectional area of the spinal cord and the APCR.
3. Reduction of the stress, which is obtained by posterior decompression surgery, improves the neurological function.
4. The severer the kyphosis was, the less the reduction of the stress was obtained after the posterior decompression surgery.

Conflict of Interest The authors declare that they have no conflict of interest.

References

1. Teresi LM, Lufkin RB, Reicher MA et al (1987) Asymptomatic degenerative disk disease and spondylosis of the cervical spine: MR imaging. Radiology 164:83–88
2. Matsumoto M, Fujimura Y, Suzuki N et al (1998) MRI of cervical intervertebral discs in asymptomatic subjects. J Bone Joint Surg Br 80:19–24

3. Bucciero A, Vizioli L, Tedeschi G (1993) Cord diameters and their significance in prognostication and decisions about management of cervical spondylotic myelopathy. J Neurosurg Sci 37:223–228
4. Fujiwara K, Yonenobu K, Hiroshima K et al (1988) Morphometry of the cervical spinal cord and its relation to pathology in cases with compression myelopathy. Spine 13:1212–1216
5. Kadanka Z, Kerkovsky M, Bednarik J et al (2007) Cross-sectional transverse area and hyperintensities on magnetic resonance imaging in relation to the clinical picture in cervical spondylotic myelopathy. Spine 32:2573–2577
6. Penning L, Wilmink JT, van Woerden HH et al (1986) CT myelographic findings in degenerative disorders of the cervical spine: clinical significance. AJR Am J Roentgenol 146:793–801
7. Ozawa H, Wu ZJ, Tanaka Y et al (2004) Morphologic change and astrocyte response to unilateral spinal cord compression in rabbits. J Neurotrauma 21:944–955
8. Scifert J, Totoribe K, Goel V et al (2002) Spinal cord mechanics during flexion and extension of the cervical spine: a finite element study. Pain Physician 5:394–400
9. Ichihara K, Taguchi T, Sakuramoto I et al (2003) Mechanism of the spinal cord injury and the cervical spondylotic myelopathy: new approach based on the mechanical features of the spinal cord white and gray matter. J Neurosurg 99:278–285
10. Kato Y, Kanchiku T, Imajo Y et al (2010) Biomechanical study of the effect of degree of static compression of the spinal cord in ossification of the posterior longitudinal ligament. J Neurosurg Spine 12:301–305
11. Ozawa H, Matsumoto T, Ohashi T et al (2001) Comparison of spinal cord gray matter and white matter softness: measurement by pipette aspiration method. J Neurosurg (Spine 2) 95:221–224
12. Ozawa H, Sato T, Hyodo H et al (2010) Clinical significance of intramedullary Gd-DTPA enhancement in cervical myelopathy. Spinal Cord 48:415–422
13. Ohshio I, Hatayama A, Kaneda K et al (1993) Correlation between histopathologic features and magnetic resonance images of spinal cord lesions. Spine 18:1140–1149
14. Matsumoto M, Ishikawa M, Ishii K et al (2005) Usefulness of neurological examination for diagnosis of the affected level in patients with cervical compressive myelopathy: prospective comparative study with radiological evaluation. J Neurosurg Spine 2:535–539
15. Seichi A, Takeshita K, Kawaguchi H et al (2006) Neurologic level diagnosis of cervical stenotic myelopathy. Spine 31:1338–1343
16. Golash A, Birchall D, Laitt RD et al (2001) Significance of CSF area measurements in cervical spondylitic myelopathy. Br J Neurosurg 15:17–21
17. Kato F, Yukawa Y, Suda K et al (2012) Normal morphology, age-related changes and abnormal findings of the cervical spine. Part II: magnetic resonance imaging of over 1,200 asymptomatic subjects. Eur Spine J 21:1499–1507
18. Suda K, Abumi K, Ito M et al (2003) Local kyphosis reduces surgical outcomes of expansive open-door laminoplasty for cervical spondylotic myelopathy. Spine 28:1258–1262
19. Hatta Y, Shiraishi T, Hase H et al (2005) Is posterior spinal cord shifting by extensive posterior decompression clinically significant for multisegmental cervical spondylotic myelopathy? Spine 30:2414–2419

Development/Plasticity/Repair

Combination of Engineered Schwann Cell Grafts to Secrete Neurotrophin and Chondroitinase Promotes Axonal Regeneration and Locomotion after Spinal Cord Injury

Haruo Kanno,[1,7] Yelena Pressman,[1] Alison Moody,[1] Randall Berg,[1] Elizabeth M. Muir,[6] John H. Rogers,[6] Hiroshi Ozawa,[7] Eiji Itoi,[7] Damien D. Pearse,[1,2,3,4] and Mary Bartlett Bunge[1,2–5]

[1]Miami Project to Cure Paralysis, [2]Department of Neurological Surgery, [3]Neuroscience Program, [4]Interdisciplinary Stem Cell Institute, and [5]Department of Cell Biology, University of Miami Miller School of Medicine, Miami, Florida 33136, [6]Department of Physiology, Development and Neuroscience, University of Cambridge, Cambridge, CB2 3EG, United Kingdom, and [7]Department of Orthopaedic Surgery, Tohoku University School of Medicine, Sendai, Japan, 9808574

Transplantation of Schwann cells (SCs) is a promising therapeutic strategy for spinal cord repair. SCs introduced into lesions support axon regeneration, but because these axons do not exit the transplant, additional approaches with SCs are needed. Here, we transplanted SCs genetically modified to secrete a bifunctional neurotrophin (D15A) and chondroitinase ABC (ChABC) into a subacute contusion injury in rats. We examined the effects of these modifications on graft volume, SC number, degradation of chondroitin sulfate proteoglycans (CSPGs), astrogliosis, SC myelination of axons, propriospinal and supraspinal axon numbers, locomotor outcome (BBB scoring, CatWalk gait analysis), and mechanical and thermal sensitivity on the hind paws. D15A secreted from transplanted SCs increased graft volume and SC number and myelinated axon number. SCs secreting ChABC significantly decreased CSPGs, led to some egress of SCs from the graft, and increased propriospinal and 5-HT-positive axons in the graft. SCs secreting both D15A and ChABC yielded the best responses: (1) the largest number of SC myelinated axons, (2) more propriospinal axons in the graft and host tissue around and caudal to it, (3) more corticospinal axons closer to the graft and around and caudal to it, (4) more brainstem neurons projecting caudal to the transplant, (5) increased 5-HT-positive axons in the graft and caudal to it, (6) significant improvement in aspects of locomotion, and (7) improvement in mechanical and thermal allodynia. This is the first evidence that the combination of SC transplants engineered to secrete neurotrophin and chondroitinase further improves axonal regeneration and locomotor and sensory function.

Key words: cell transplantation; chondroitinase; glial scar; Schwann cell; spinal cord injury

Introduction

Repair of spinal cord injury (SCI) in adult mammals is challenging due to multiple factors, including extensive cell loss, axonal disruption, growth inhibitory molecules in the scar, and lack of growth-promoting molecules (Schwab and Bartholdi, 1996; Fawcett and Asher, 1999; Silver and Miller, 2004). Accordingly, treatments to overcome these multiple deficits will require a multifaceted combination strategy (Bunge, 2008; Fortun et al., 2009).

Received June 18, 2013; revised Nov. 14, 2013; accepted Dec. 19, 2013.

Author contributions: H.K., Y.P., E.M.M., J.H.R., H.O., E.I., D.D.P., and M.B.B. designed research; H.K., Y.P., A.M., R.B., and M.B.B. performed research; H.K., Y.P., E.M.M., and J.H.R. contributed unpublished reagents/analytic tools; H.K., Y.P., A.M., R.B., and M.B.B. analyzed data; H.K., D.D.P., and M.B.B. wrote the paper.

This work was supported by the National Institutes of Health (Grant 09923 to M.B.B. and Grant 056281 to D.D.P.), the Miami Project to Cure Paralysis and the Buoniconti Fund (to M.B.B.), and the Uehara Memorial Foundation (Research Fellowship Grant 2010 to H.K.). We thank Dr. Dalton Dietrich for arranging H.K.'s visit at the Miami Project, the Animal Core of the Miami Project for help with animal care, the Viral Vector Core for expanding virus, the Imaging Core for help with confocal microscopy, and Acorda Therapeutics for suggesting the DMB assay.

The authors declare no competing financial interests.

Correspondence should be addressed to Haruo Kanno, MD, PhD, Department of Orthopaedic Surgery, Tohoku University School of Medicine, 1-1 Seiryo-machi, Aoba-ku, Sendai, 9808574, Japan. E-mail: kanno-h@med.tohoku.ac.jp.

DOI:10.1523/JNEUROSCI.2661-13.2014

 0270-6474/14/341838-18$15.00/0

Our previous studies demonstrated that transplantation of Schwann cells (SCs) holds promise for SCI repair (Xu et al., 1997; Takami et al., 2002; Pearse et al., 2004; Fouad et al., 2005; Golden et al., 2007; Pearse et al., 2007; Bunge, 2008; Fortun et al., 2009; Tetzlaff et al., 2011). The transplantation of SCs provides neuroprotection, reduces cyst formation, promotes axonal regrowth and myelination, and modestly improves functional outcome. *In vitro* systems to harvest and expand human SCs present a unique opportunity for autologous transplantation after human SCI (Levi et al., 1995; Rutkowski et al., 1995; Bunge and Pearse, 2003; Bunge and Wood, 2012).

We previously investigated combining SC transplantation with a bifunctional neurotrophin, D15A, for contusion injury (Golden et al., 2007). D15A activates both TrkB and TrkC receptors and thus mimics the effects of NT-3 and BDNF (Urfer et al., 1994; Cao et al., 2005). Transduced SCs secreting D15A markedly increased SCs and axons in the transplant and myelination of the axons in the transplant (Golden et al., 2007). SCs secreting D15A, however, did not lead to improvement in open field locomotion (on the basis of BBB scoring; Basso et al., 1995), possibly because they did not enable regenerated axons to leave the transplant.

Chondroitin sulfate proteoglycans (CSPGs) are synthesized and deposited in the glial scar after SCI (Lemons et al., 1999; Plant et al., 2001; Morgenstern et al., 2002; Jones et al., 2003; Tang et al., 2003). CSPGs are known to inhibit regeneration of axons and contribute to the limited functional recovery observed after SCI. Degradation of CSPGs with chondroitinase ABC (ChABC) promotes axonal regeneration and functional recovery (Bradbury et al., 2002; Silver and Miller, 2004; Fouad et al., 2005; Barritt et al., 2006; Cafferty et al., 2007; Massey et al., 2008; Bradbury and Carter, 2011). ChABC, an enzyme that cleaves glycosaminoglycan side chains from the CSPGs, is useful for overcoming the inhibitory influence of CSPGs on axon growth in the injured spinal cord (Bradbury et al., 2002).

We predicted, therefore, that combining SC transplantation with neurotrophin and ChABC to increase axons, not only growing into the graft but also exiting the graft, would improve locomotor function after SCI. Accordingly, we transplanted genetically engineered SCs to secrete D15A and ChABC into a rat contusion injury and investigated the graft volume, SC number, degradation of CSPGs, astrogliosis, SC myelination of axons, presence of propriospinal and supraspinal axons, locomotor outcome, and hind paw mechanical and thermal sensitivity. Engineering of SCs to secrete neurotrophin and ChABC significantly promoted axonal regeneration and improved locomotor and sensory outcomes, the combination being more efficacious than either treatment alone.

Materials and Methods

Reagents. Antibodies used were as follows: mouse anti-neurofilament antibody (RT97; Developmental Studies Hydridoma Bank, Iowa City, IA), rabbit anti-S100 antibody (catalog #119250; Dako), chicken anti-GFP antibody (catalog #P42212; Millipore), rabbit anti-mCherry antibody (catalog #632496; Clontech), mouse anti-CS56 antibody (catalog #C8035; Sigma-Aldrich), mouse anti-2B6 antibody (catalog #270432; Seikagaku), mouse anti-GFAP antibody (catalog #SMI-22R; Covance), and rabbit anti-5-HT antibody (catalog #20080; Immunostar). Secondary antibodies included goat anti-chicken IgG Alexa Fluor 488 antibody (catalog #A-11039), goat anti-rabbit IgG Alexa Fluor 594 antibody (catalog #A-11012), goat anti-mouse IgG Alexa Fluor 405 antibody (catalog #A-31553), goat anti-rabbit IgG Alexa Fluor 405 antibody (catalog #A-31556), goat anti-rabbit IgG Alexa Fluor 660 antibody (catalog #A-21073), and goat anti-mouse IgG Alexa Fluor 660 antibody (catalog #A-21054), all from Invitrogen. Purified ChABC (catalog #100332) was from Seikagaku, chondroitin sulfate (catalog #C4384) and dimethylmethylene blue (DMB; catalog #341088) were from Sigma-Aldrich, and the NT-3 ELISA kit (catalog #G7641) was from Promega.

Schwann cells. Purified populations of SCs were obtained from the sciatic nerves of adult female Fischer rats (Harlan Laboratories) as described previously (Morrissey et al., 1991). SCs were then purified and expanded as described previously (Meijs et al., 2004). Briefly, after removal of the epineurium, the nerves were cut into 3-mm-long segments that were placed into 60 mm plastic culture dishes and covered with D10 medium (DMEM; Invitrogen) containing 10% fetal bovine serum (Hyclone). The segments were transferred to new dishes weekly and the medium was refreshed biweekly. After 2 weeks, the explants were treated with dispase (Roche) and collagenase (Worthington), dissociated and, after centrifugation (1500 *g* at 4°C), resuspended in D10 medium with the SC mitogens, pituitary extract (20 μg/ml; Biomedical Technologies), forskolin (2 μM; Sigma-Aldrich), and heregulin (2.5 nM; Genentech). The cells were then plated onto poly-L-lysine-coated culture dishes (Sigma-Aldrich), given fresh medium biweekly, and, when confluent, replated at 1/4 confluent density into new dishes. Early on, the cells were treated with Thy-1 and rabbit complement (MP Biomedicals) to eliminate remaining fibroblasts. The cells were grown to confluency and passaged to new dishes three times (P3) before transplantation. The resulting SC cultures were >95% pure based on S100 immunostaining (Dako; Takami et al., 2002).

Lentiviral vector preparation. Lentiviral vectors encoding enhanced GFP and mCherry were used to transduce the SCs to enable their tracking *in vivo* (Golden et al., 2007; Hill et al., 2007; Pearse et al., 2007; Patel et al., 2010). Lentiviral vector preparation was performed as described previously (Follenzi et al., 2000). The genes were subcloned into a lentiviral vector plasmid containing the cytomegalovirus promoter and the Woodchuck posttranscriptional regulatory element.

The lentiviral particles were produced by the Miami Project Viral Vector Core. Cultured HEK 293T cells were used for transfecting the plasmids and viral harvesting. Briefly, 24 h before transfection, HEK 293T cells were plated in T-175 flasks (using 25 ml of high-glucose DMEM plus 10% FBS) so that the cells reached 90% confluency on the day of transfection. For each flask, dilute 12.2 μg of transfer vector, 6.1 μg of pMDL (Gag/Pol), 3.1 μg of pREV, 3.7 μg of vesicular stomatitis virus glycoprotein (pVSVG) were combined in 1 ml of Opti-MEM I Reduced Serum Medium. Lipofectamine 2000 was mixed before use, then diluted to 62.5 μl in 1 ml of Opti-MEM I Reduced Serum Medium and incubated for 5 min. The diluted DNA was combined with diluted Lipofectamine 2000 and incubated for 20 min at room temperature. The complexes were added to the flask and incubated at 37°C in a CO_2 incubator overnight. After 40 h in 30 ml of fresh medium, the supernatant was harvested and centrifuged at 500 × g for 5 min at 4°C, followed by filtration using a 0.45-μm-pore PVDF Durapore filter (Millipore). The supernatant was then ultracentrifuged at 21,000 rpm for 2.5 h at 4°C in a SW-28 rotor (Beckman). The virus pellets were resuspened in PBS/1% BSA. The viral titer was determined by p24 ELISA assay (PerkinElmer) for quantifying p24 core protein concentrations. Purified viral vector stocks were stored at −80°C until SC infection.

Human D15A cDNA was generated previously (Urfer et al., 1994). The lentiviral vector encoding D15A was prepared as described previously (Follenzi and Naldini, 2002; Blits et al., 2005; Golden et al., 2007). The gene for *Proteus vulgaris* chondroitinase ABC expression in mammalian cells was developed by Muir et al. (2010). Lentiviral vectors encoding the ChABC gene were generated by the Verhaagen team (Hendriks et al., 2007; Zhao et al., 2011).

Lentiviral vector transduction of Schwann cells. These vectors were used to transduce SCs at passage one. SC cultures were transduced by the addition of a predetermined volume of the concentrated lentivirus. SCs (5×10^5/well) at 70% confluency were seeded in 12-well plates with D10 and mitogens and then transduced overnight with varying multiplicities of infection (MOIs; 10, 20, 30, 50, 100, and 2000) of lentiviral vectors. The following day, medium was refreshed and the cultures were incubated for 2 more days. The cell cultures were fixed in 4% paraformaldehyde and stained with Hoechst to allow a comparison of Hoechst-labeled nuclei and GFP- or mCherry-positive cells. The *in vitro* transduction efficiency lentiviral system was assayed using GFP and mCherry expressions of SCs. An optimal MOI of 30 was designated by highest transduction efficiency (>95% of GFP- or mCherry-positive cells) with no obvious signs of toxicity. The optimal MOI was used for all subsequent *in vitro* and *in vivo* studies.

We prepared four different types of transduced SCs: (1) with only GFP (GFP-SCs); (2) with only mCherry (mCherry-SCs), (3) with GFP and D15A (GFP/D15A-SCs), and (4) with mCherry and ChABC (mCherry/ChABC-SCs). GFP and mCherry lentiviral vectors were used to visualize the SCs transduced with D15A or ChABC separately. The transduced cells, harvested and stored in liquid nitrogen, were thawed and expanded as needed.

D15A activity in vitro. D15A levels in conditioned medium were determined using an NT-3 ELISA capable of recognizing the NT-3 backbone of D15A. SCs were thawed and incubated in growth medium. Conditioned media from GFP- or GFP/D15A-transduced SC or nontransduced SC cultures were collected at 24 h intervals. The amount of neurotrophin was determined according to the manufacturer's protocol (Promega). Neurite outgrowth assays were used to demonstrate D15A bioactivity (Golden et al., 2007). Lumbar dorsal root ganglia (DRG) were removed on embryonic day 15 and placed in 12-well dishes. Then, 600 μl of conditioned medium collected from confluent GFP-SC or GFP/

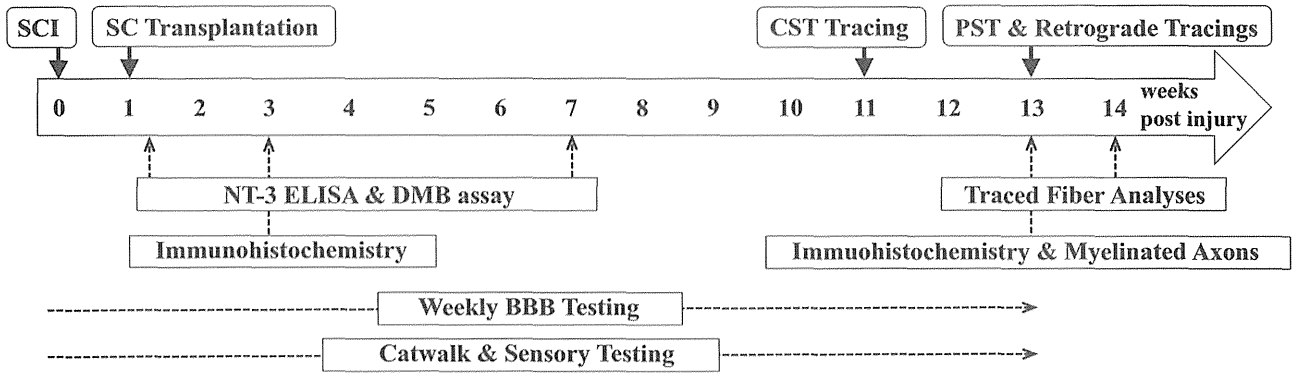

Figure 1. Summary of the experimental timeline.

D15A-SC cultures at 24 h intervals or medium supplemented with BDNF (730 ng/ml) and NT-3 (730 ng/ml) were added to the wells for 3 d at 37°C in 5% CO_2. Each culture was fixed and immunostained with a mouse monoclonal anti-neurofilament antibody (RT97, 1:5 in TBS–normal goat serum; Developmental Studies Hydridoma Bank).

Chondroitinase ABC activity in vitro. The enzymatic activity of ChABC in SC-conditioned media was quantified by a DMB (Sigma-Aldrich) assay that measured the sulfated glycosaminoglycan cleaved by ChABC (Farndale et al., 1982; Ettenson et al., 2000; Liu et al., 2012). For the DMB assay, 10 μl of conditioned medium were collected daily from nontransduced SC-, mCherry-, or mCherry/ChABC-transduced SC cultures and incubated with 10 μl of chondroitin sulfate (0.25 mg/ml) for 15 min at 37°C. As described previously (Liu et al., 2012), 180 μl of DMB solution (16 mg of DMB, 2.37 g of NaCl, 3.04 g of glycine, 75 ml of 0.1 M HCl in 1 L of H_2O) were added to 20 μl of the reaction sample and the absorbance was recorded at 660 nm. The absorbance of the chondroitin sulfate without the conditioned medium was used as the control. The enzymatic activity was calculated with a linear standard curve generated using purified ChABC (Seikagaku).

To confirm ChABC bioactivity to degrade CSPGs in normal spinal cord tissue, cryostat sections were incubated in PBS, in conditioned medium collected from mCherry/ChABC-transduced SC cultures, or in PBS containing ChABC (300 mU/ml) for 3 h at 37°C (Moon et al., 2002). Immunostaining of the incubated sections for CS-56 (to detect intact CSPGs) and 2B6 (to detect degraded CSPGs) was performed as described in Immunohistochemistry, below.

Animals. Adult female Fischer rats (total $n = 280$; 160–180 g weight; Harlan Laboratories) were housed in accordance with National Institutes of Health guidelines and the *Guide for the Care and Use of Laboratory Animals*. The Institutional Animal Care and Use Committee of the University of Miami approved all animal procedures. Efforts were made to minimize the number of animals used and to decrease animal suffering. Rats were anesthetized (45 mg/kg ketamine, 5 mg/kg xylazine) by intraperitoneal injection. Adequate anesthesia was determined by monitoring the corneal reflex and hindlimb withdrawal to painful stimuli. During surgery, the rats were kept on a heating pad to maintain body temperature at 37 ± 0.5°C. Rats were housed two per cage at a temperature of 24°C with *ad libitum* access to water and food before and after surgery. Figure 1 summarizes the experimental timeline in this study.

Contusion injury. A laminectomy was performed at thoracic vertebra T8, exposing the dorsal surface of the spinal cord without disrupting the dura mater. Moderate thoracic spinal cord contusion injuries (10 g weight dropped 12.5 mm) were induced using the MASCIS weight-drop device (Gruner, 1992). Animals were excluded immediately when the height or velocity errors exceeded 7% or if the compression distance was not within the range of 1.35–1.75 mm (Barakat et al., 2005; Pearse et al., 2007). After injury, the overlying musculature was sutured and the skin closed using wound clips. The rats recovered in a warmed cage with water and food easily accessible. The rats received postoperative care that included the administration of gentamicin (5 mg/kg, intramuscular; Abbott Laboratories), Buprenex (0.3 mg/kg, subcutaneous; Reckitt Benckiser), and lactated Ringer's solution (Pearse et al., 2007). Bladders were expressed twice a day until spontaneous voiding began.

Table 1. Listing of the experimental groups and the transplanted SCs

Experimental groups[a]	GFP-SCs	GFP/D15A-SCs	mCherry-SCs	mCherry/ChABC-SCs
DMEM/F12	—	—	—	—
SC control	+	—	+	—
SC-D15A	—	+	+	—
SC-ChABC	+	—	—	+
SC-D15A + ChABC	—	+	—	+

[a]Two types of transduced SCs (1×10^6 cells for each type; total of 2×10^6) were mixed and transplanted in each experimental group. The number of D15A- or ChABC-transduced SCs transplanted in the SC-D15A and SC-ChABC groups were the same in the combination group.

SC transplantation. Transduced SCs were harvested from culture by trypsinization, centrifuged, resuspended, and counted. SCs were resuspended in aliquots of DMEM/F12 medium (Live Technologies). The two types of transduced SCs were mixed just before transplantation. Animals were randomly assigned to one of five transplant groups ($n = 56$ per group): (1) DMEM/F12 medium alone (DMEM/F12 group), (2) mCherry-SCs + GFP-SCs (SC control group), (3) mCherry-SCs + GFP/D15A-SCs (SC-D15A group), (4) GFP-SCs + mCherry/ChABC-SCs (SC-ChABC group), and (5) GFP/D15A-SCs + mCherry/ChABC-SCs (SC-D15A + ChABC group; Table 1). At 7 d after injury, rats were reanesthetized, the injury site was exposed, and a total of 2×10^6 SCs (1×10^6 cells for each type) in 6 μl of DMEM/F12 medium was injected into the contused area (Takami et al., 2002; Pearse et al., 2004). The SC injection was performed over 3 min (2 μl/min) into the injury epicenter at a depth of 1 mm in the midline at T8 using a micromanipulator with a microinjector (World Precision Instruments; Patel et al., 2010). A 10 μl Hamilton syringe with a pulled glass capillary tube [150 μm inner diameter (ID)] was secured in the micromanipulator. The capillary tube was kept in place for an additional 3 min to minimize leakage upon withdrawal (Patel et al., 2010). After injection, the muscle layers were sutured and the skin closed with wound clips. Table 2 summarizes number of animals in each group used for each analysis in this study.

Tracing. Three tracing experiments were performed, each one in a separate cohort of animals. For corticospinal tract (CST) anterograde tracing at 11 weeks after contusion, biotinylated dextran amine (BDA; 10,000 MW, 10% in PBS, 0.5 μl/site; Invitrogen) was stereotactically injected into 6 sites in the sensorimotor cortex (0.7, 1.4, 2.5 mm posterior to the bregma, ±2.3 mm lateral to the midline, depth 1.5 mm; Hill et al., 2001). The injections, made with a glass tube (50 μm ID) attached to a 10 μl Hamilton syringe held in the micromanipulator, were performed over 5 min. For propriospinal tract (PST) anterograde tracing, at 13 weeks after injury, a laminectomy was performed at T6. BDA (0.15 μl/site) was stereotactically injected into 4 sites bilaterally (7.0 and 5.5 mm rostral to the rostral edge of the injury, ±0.3 mm lateral to the midline, 1.5 mm beneath the cord surface). The injections with a 1 μl syringe and glass tube (150 μm ID) were performed over 3 min in a micromanipulator. For retrograde neuronal tracing, animals at 13 weeks after injury received

Table 2. Number of animals for each experimental analysis at each time point[a]

Experimental group	Immunohistochemistry, (3 wk, 13 wk)[b]	Myelinated axons[b] (13 wk)	NT-3 ELISA in vivo (9 d, 3 wk, 7 wk)	DMB assay in vivo (9 d, 3 wk, 7 wk)	CST tracing (14 wk)	PST tracing[c] (14 wk)	Retrograde tracing[c] (14 wk)
DMEM/F12	6, 6	5	4, 4, 4	3, 3, 3	6	5	7
SC control	6, 6	5	4, 4, 4	3, 3, 3	6	5	7
SC-D15A	6, 6	5	4, 4, 4	3, 3, 3	6	5	7
SC-ChABC	6, 6	5	4, 4, 4	3, 3, 3	6	5	7
SC-D15A + ChABC	6, 6	5	4, 4, 4	3, 3, 3	6	5	7

[a]Numbers in parentheses indicate time points of analyses after injury.

[b]Seven animals of those observed until 12 weeks were used for BBB scoring.

[c]Seven animals were used for analyses of Catwalk and allodynia.

a laminectomy at T10. A total of 0.6 μl of 2% fast blue (FB, 0.3 μl/site; Sigma-Aldrich) was injected into two sites in the spinal cord bilaterally at 7 mm caudal to the caudal edge of the injury (Takami et al., 2002; Pearse et al., 2004). Every injection was performed over a 3 min period and the injection needle was kept in place for an additional 3 min to minimize leakage upon withdrawal (Xu et al., 1999; Chau et al., 2004).

Immunohistochemistry. At 2 or 12 weeks after transplantation, animals were transcardially perfused with normal saline, followed by 4% paraformaldehyde in 0.1 M PBS at pH 7.4 (Takami et al., 2002). The T7–9 spinal cord segments centered at the injury site were postfixed in the same fixative overnight at 4°C, cryoprotected in 30% sucrose in PBS for 48 h at 4°C, and embedded in gelatin (Oudega et al., 1994). Serial sagittal cryostat sections (20 μm thick) were mounted on slides. Sections were rinsed 3× with TBS and incubated in a blocking solution of 5% NGS with 0.5% Triton X-100 for 1 h at room temperature. The sections were incubated in antibodies against chicken anti-GFP (1:500), rabbit anti-mCherry (1:500), mouse anti-CS56 (1:500), mouse anti-2B6 (1:200), mouse anti-GFAP (1:500), or rabbit anti-5-HT (1:2000) diluted in TBS with 5% NGS and 0.5% Triton X-100 overnight. Sections were rinsed 3× with TBS and incubated with secondary antibodies (all 1:200; Invitrogen), goat anti-chicken IgG Alexa Fluor 488, goat anti-rabbit IgG Alexa Fluor 594, goat anti-mouse IgG Alexa Fluor 405, goat anti-rabbit IgG Alexa Fluor 405, goat anti-rabbit IgG Alexa Fluor 660, or goat anti-mouse IgG Alexa Fluor 660, with 1% NGS and 100 μM Hoechst dye (Sigma-Aldrich) for 1 h at room temperature. Sections were rinsed 3× with TBS and coverslipped with Vectashield (Vector Laboratories).

Graft volume and SC number. SC graft volume was analyzed in the serial sagittal sections that were immunostained for GFP and mCherry using unbiased computer-assisted microscopy and StereoInvestigator 10 software (MBF Bioscience; Golden et al., 2007; Patel et al., 2010). The SC graft in each section (20 μm thickness, 200 μm intervals) was delineated at 20× using GFP and mCherry fluorescence and immunolabeling to determine the SC graft area. This area was automatically calculated and the graft volume determined using the equation: $V = \sum$ [transplant area × section thickness × 10 (number of sections in each sampling interval)] (Biernaskie et al., 2007). The graft area in each section was measured blindly. Then two serial sagittal sections that contained the lesion site with the largest graft area were blindly selected for other analyses.

To compare the numbers of transplanted labeled SCs in the experimental groups, the serial sections (20 μm thickness, 200 μm intervals) were analyzed using StereoInvestigator software (Patel et al., 2010). SC transplants were outlined at 4× and then SCs were counted under a 63× oil objective. Then the optical fractionator sampling design (counting frame area, 50 × 50 μm; sampling grid size, 250 × 250 μm) was used. In each sampling site, both GFP- and mCherry-labeled SCs were marked and recorded using a dissector probe, only counting the labeled cell bodies that contained a nucleus. SC number within the transplant in the section was automatically calculated by StereoInvestigator software. Two serial sagittal sections per rat around the midline containing the largest graft were chosen and then the number of SCs in the two sections were summed and compared among the groups.

D15A activity in vivo. At 2 d or 2 or 6 weeks after transplantation, spinal cord segments (5 mm length) centered at the injury/graft sites were removed, quickly frozen, and stored at −80°C. Tissue was weighed and homogenized by placing it in 10× weight/volume lysis buffer (137 mM NaCl, 20 mM Tris, 1% NP-40; Calbiochem), 10% glycerol, 1 mM phenylmethylsulfonyl fluoride, 0.5 mM sodium vanadate, 1 μg/ml leupeptin, and 10 μg/ml aprotinin, pH 8.0. Samples were centrifuged at 12,000 rpm for 5 min and the supernatants harvested and stored at −80°C. The amount of neurotrophin in the supernatants was determined using an ELISA recognizing NT-3 according to the manufacturer's protocol (Ying et al., 2003; Golden et al., 2007). Measurements were normalized to total protein, as determined by a standardized Bradford protein assay. NT-3 was expressed as the total amount in the sample per milligram of total protein.

Chondroitinase ABC activity in vivo. To analyze cleavage of CSPGs by ChABC in the transplanted spinal cord, immunointensity of CS56 and 2B6 antibody staining was quantified in the two serial sagittal sections around the midline containing the largest grafts (Karimi-Abdolrezaee et al., 2010). Quantification of immunointensity of GFAP staining was also performed to analyze astrogliosis. The entire sagittal section was imaged at 10× using a confocal microscope with tiling and stitching software (Fluoview, Olympus America). For imaging, the appropriate confocal setting in the first microscopy session that would avoid signal saturation was determined and the same setting was used thereafter. Using ImageJ software, the obtained images were converted into gray scale and the 5 mm length of spinal cord containing lesion and perilesion areas was traced in each section. Furthermore, automatic thresholding for each image was performed using the software to determine the threshold for a specific signal (Karimi-Abdolrezaee et al., 2010). The default threshold setting was used and the thresholding values were maintained at constant levels for all analyses. After setting the threshold, the integrated immunodensity above the threshold was automatically calculated. Then, the integrated density was divided by the sample area to calculate the mean density per unit area. This calculation was performed to compensate for the different sizes of the region of interest in the spinal cord. The mean values for each animal were then compared.

To analyze enzymatic activity of ChABC in the transplanted spinal cord, a DMB assay was performed using the supernatants from the homogenized tissue (see Chondroitinase ABC activity *in vitro*, above). 10 μl of supernatant were incubated with 10 μl of chondroitin sulfate (0.25 mg/ml) for 15 min at 37°C using an absorbance of 660 nm. Measurements, calculated with a linear standard curve, were normalized to total protein determined by a standardized Bradford protein assay.

SC migration. The migration of GFP- and mCherry-positive SCs into the host spinal cord was quantified. First, the sections that contained transplanted SCs were immunostained for GFAP to define the border between the host spinal cord tissue (GFAP-positive) and the lesion site/implant (GFAP-negative). After tracing these borders, the GFP- and mCherry-positive SCs in the host spinal cord were automatically counted using the particle analysis tool of ImageJ (Petryniak et al., 2007; Drury et al., 2011). The counts were performed on the two serial sagittal sections around the midline containing the largest transplants and compared among the groups.

SC-myelinated axon counts. A 1 mm transverse slice from the graft/injury center was removed after perfusion and prepared for electron microscopy (Xu et al., 1995). Then, 1 μm plastic transverse sections were stained with toluidine blue, followed by 4% paraphenylenediamine to visualize myelin (Murray et al., 2001). SC-myelinated axons were counted at 63× under oil; the total number was obtained with StereoInvestigator software (MBF Bioscience; Takami et al., 2002; Pearse et al., 2004; Golden et al., 2007). Using the optical fractionator sampling design

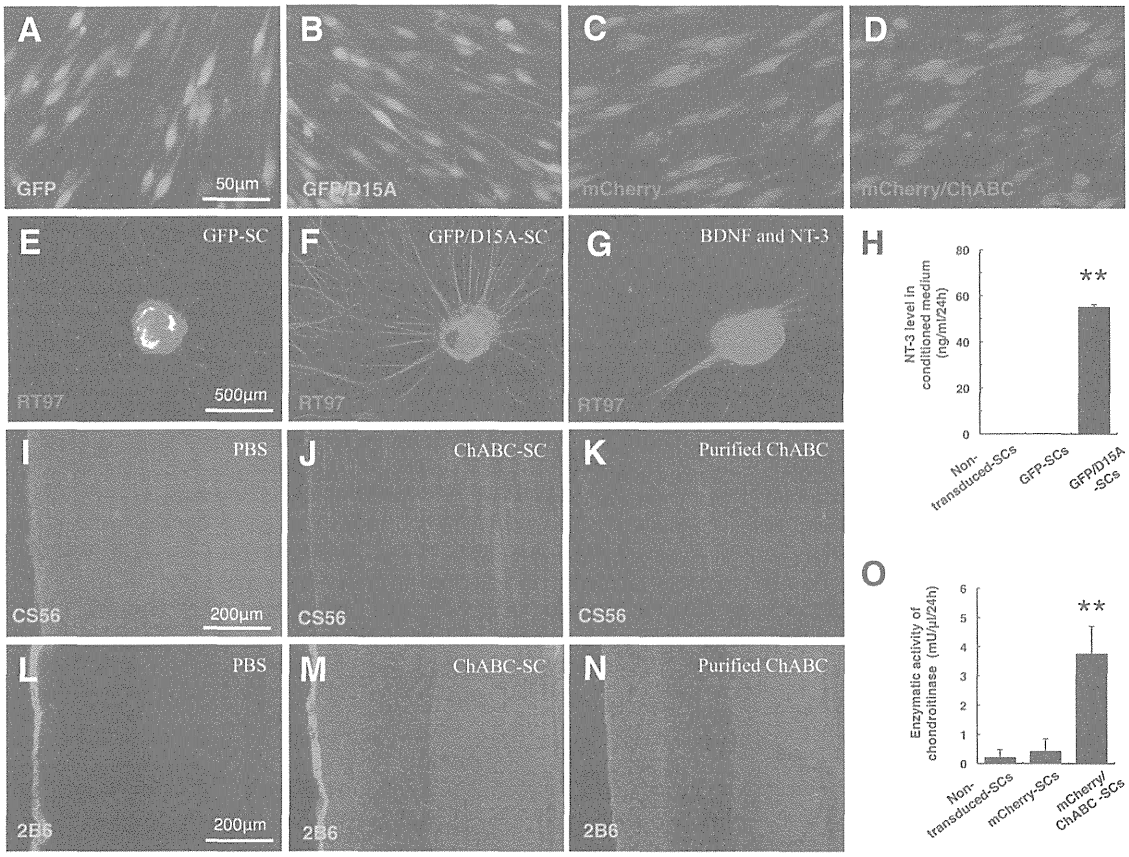

Figure 2. Transduced SCs secrete bioactive D15A and ChABC *in vitro*. ***A–D***, SCs transduced to express GFP, GFP/D15A, mCherry, and mCherry/ChABC showed good expression of GFP or mCherry and morphological differences were not observed. ***E–G***, Embryonic DRG incubated in conditioned medium from a D15A/GFP-SC culture (***F***) and in medium containing added BDNF and NT-3 (***G***) showed robust neurite outgrowth compared with GFP-SC conditioned medium (***E***). ***H***, NT-3 ELISA revealed that NT-3 levels in conditioned medium from GFP/D15A-SC cultures were significantly higher than from nontransduced SC and GFP-SC cultures. ***I–K***, After CS56 staining, immunoreactivity in the spinal cord sections incubated with conditioned medium from a ChABC-transduced SC culture (***J***) and purified ChABC (***K***) was decreased compared with PBS (***I***). ***L–N***, Conversely, after 2B6 staining, immunoreactivity in the sections incubated with the conditioned medium (***M***) and purified ChABC (***N***) was increased compared with PBS (***L***). ***O***, DMB assay demonstrated enzymatic activity of ChABC in conditioned medium from mCherry/ChABC-SC cultures. Data are presented as mean ± SEM; $n = 3$ per each SC group. $^{**}p < 0.01$.

(counting frame area, 50 × 50 μm; grid size, 150 × 150 μm), the graft epicenter was systematically sampled. These sections allow central (oligodendrocyte) myelin to be distinguished morphologically from peripheral (SC) myelin (Bunge et al., 1994; Pearse et al., 2004). The analysis was performed by the examiners blinded to the animal groups.

Quantitation of traced axons and brainstem neurons. Fourteen weeks after injury, the rats were transcardially perfused and the brains and spinal cords containing the injury site were extirpated and embedded in gelatin. Serial 40-μm-thick transverse sections of the brainstem and sagittal sections of the spinal cord were prepared.

For quantitation of CST anterograde tracing, BDA-labeled axons were examined in every fifth sagittal section (40 μm thickness, 200 μm intervals). The labeled axons were visualized with fluorescein-conjugated streptavidin (Invitrogen; Pearse et al., 2004) and the sections coverslipped with Citifluor (UKC Chemical Laboratory). Numbers of BDA-labeled axons were determined by counting all labeled axons crossing imaginary lines placed perpendicular to the rostral-caudal axis of the spinal cord at 500 μm rostral and 500 μm caudal to the edges of the graft (delineated by GFP- and mCherry-labeled SCs) and through the center of the graft (Pearse et al., 2004). BDA-labeled axons in host tissue outside the graft epicenter were counted separately. The numbers in each section were summed per rat and then multiplied by 5 to obtain the final number.

For quantitation of PST anterograde tracing, BDA-labeled axons were counted using the sagittal sections and visualized as above. The number of BDA-labeled propriospinal axons was determined at the center of the graft and at 500 μm caudal to the caudal edge of the graft (Chau et al., 2004). We selected the two serial sagittal sections (40 μm thickness, 200 μm intervals) around the midline that contained the largest implant per rat and the numbers of axons in the two sections were summed and compared.

To assess numbers of neurons labeled by retrograde tracing, every tenth section (40 μm thickness, 400 μm intervals) of the embedded brainstems was identified according to Paxinos and Watson (1998). The number of FB-labeled neurons was quantified in the reticular formation, the raphe nuclei, and the entire brainstem (Takami et al., 2002; Pearse et al., 2004; Lo et al., 2009). Only neurons containing nuclei were counted (Iannotti et al., 2003; Carter et al., 2011). These numbers were summed per rat and multiplied by 10 to obtain the total number of labeled neurons for each region.

Quantitation of 5-HT-immunolabeled axons. The number of 5-HT-immunolabeled axons was determined by counting all labeled axons crossing imaginary lines placed perpendicular to the rostral-caudal axis of the spinal cord at the center of the graft and at 500 μm caudal to the caudal edge of the graft (Pearse et al., 2004). For comparing the numbers of axons among the five groups, the two serial sagittal sections around the midline that contained the largest graft per rat were selected; the numbers of axons in these sections were summed and compared.

BBB open-field testing and Catwalk analysis. All locomotor assessments were performed by at least two examiners blinded to the group allocation. BBB scoring (Basso et al., 1995) was performed weekly from 1 to 13 weeks after injury. In addition, a BBB subscore was obtained to provide a separate assessment of hindlimb and tail positioning (Basso, 2004). All animals in the present study scored 21 for the BBB score and 13 for the

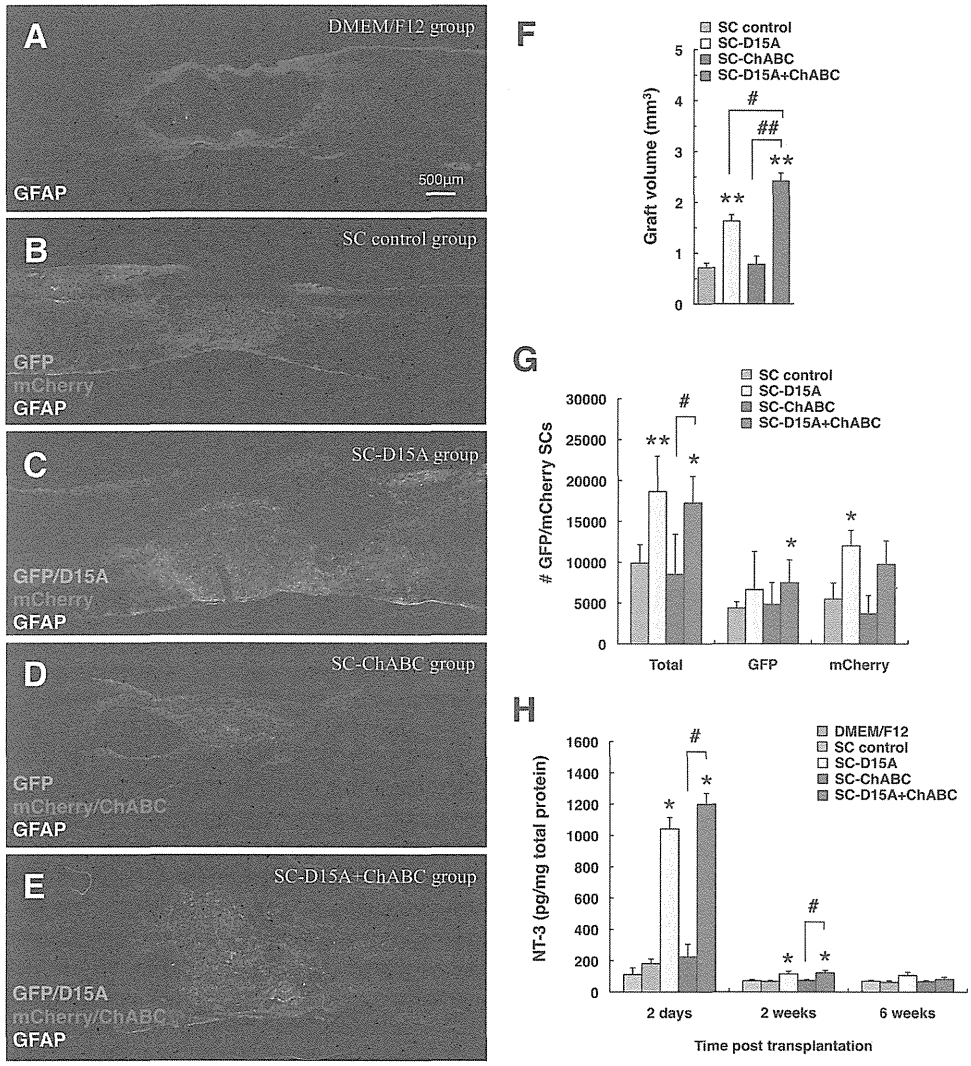

Figure 3. D15A increases graft volume and SC number in the injured spinal cord. ***A–E***, At 12 weeks after transplantation, GFP-labeled (green) and mCherry-labeled (red) SCs had mixed well and were present in all transplanted groups. The groups with D15A (***C*** and ***E*** vs ***B*** and ***D***) showed larger SC grafts. ***F***, Quantitation of the graft volume. ***G***, Comparison of total numbers of labeled SCs. ***H***, NT-3 ELISA of transplanted spinal cord tissue samples. Data are presented as mean ± SEM; $n = 5$ per group in ***F*** and ***G***; $n = 4$ per group in ***H***. $^{*}p < 0.05$, $^{**}p < 0.01$ compared with SC control group. $^{\#}p < 0.05$, $^{\#\#}p < 0.01$ compared with SC-D15A or SC-ChABC group.

BBB subscore during baseline assessment. Catwalk gait analysis evaluates both static and dynamic locomotor parameters, such as stride length, base of support, interlimb coordination, and swing/stance phases (Hamers et al., 2001; Koopmans et al., 2005). The objective analyses using Catwalk can overcome the disadvantage of a more subjective assessment of coordination by the BBB locomotor rating scale (Hamers et al., 2001; Deumens et al., 2007). At 1 week before injury, the animals were trained to cross the walkway a minimum of 3× daily for Catwalk analysis. Catwalk data were obtained before injury and at 5, 9, and 13 weeks after injury; a minimum of three uninterrupted crossings/animal was required. Stride length, base of support, and interlimb coordination were analyzed by making use of the regularity index and frequency of regular steps (% Ab step pattern; Cheng et al., 1997; Lankhorst et al., 2001; Joosten et al., 2004).

Assessment of mechanical and thermal allodynia. Assessment of mechanical and thermal allodynia was done in a blinded manner before injury and at 5, 9, and 13 weeks after injury. For mechanical allodynia testing, rats were placed in elevated Plexiglas chambers with a wire mesh floor and allowed 30 min to acclimatize. Cutaneous sensitivity to innocuous mechanical stimulation of both hindpaws was evaluated using the up-down method with eight specific calibrated von Frey filaments (Chaplan et al., 1994). A von Frey filament was pressed against the plantar skin such that it slightly bowed. If no hindpaw withdrawal was elicited, then the next higher force filament was used. A hindpaw withdrawal indicated the use of a filament with a lesser force. Both hindpaws were tested ~5 min apart. The series of responses to the filaments was converted into a 50% withdrawal threshold measured in grams (Chaplan et al., 1994); the highest withdrawal threshold was 15 g and the lowest was 0.25 g. To be included in the study, a withdrawal threshold of 4 g or less was required (Hama and Sagen, 2011).

For thermal allodynia testing, a rat was placed in a Plexiglas enclosure that rested on an elevated glass floor. A commercially available infrared plantar test device (Ugo Basile) was used to assess sensitivity of the plantar hindpaws to a brief noxious heat stimulus (Hargreaves et al., 1988). After acclimatization for 30 min, an infrared emitter under the glass floor was positioned directly beneath the midplantar hindpaw. The length of time between the onset of the infrared stimulus and the paw withdrawal is termed "withdrawal latency" (measured in seconds). The device shuts off the infrared stimulus automatically and records the withdrawal latency when an animal withdraws the hindpaw from the stimulus. The average of three trials/paw was used to report the final withdrawal latency. Testing of the same paw was separated by at least 5 min. To prevent tissue damage, a cutoff of 20 s was used (Hama et al., 2010).

Statistical analysis. All statistical analyses were performed using the GraphPad Prism 5.0a software program. All data are presented as

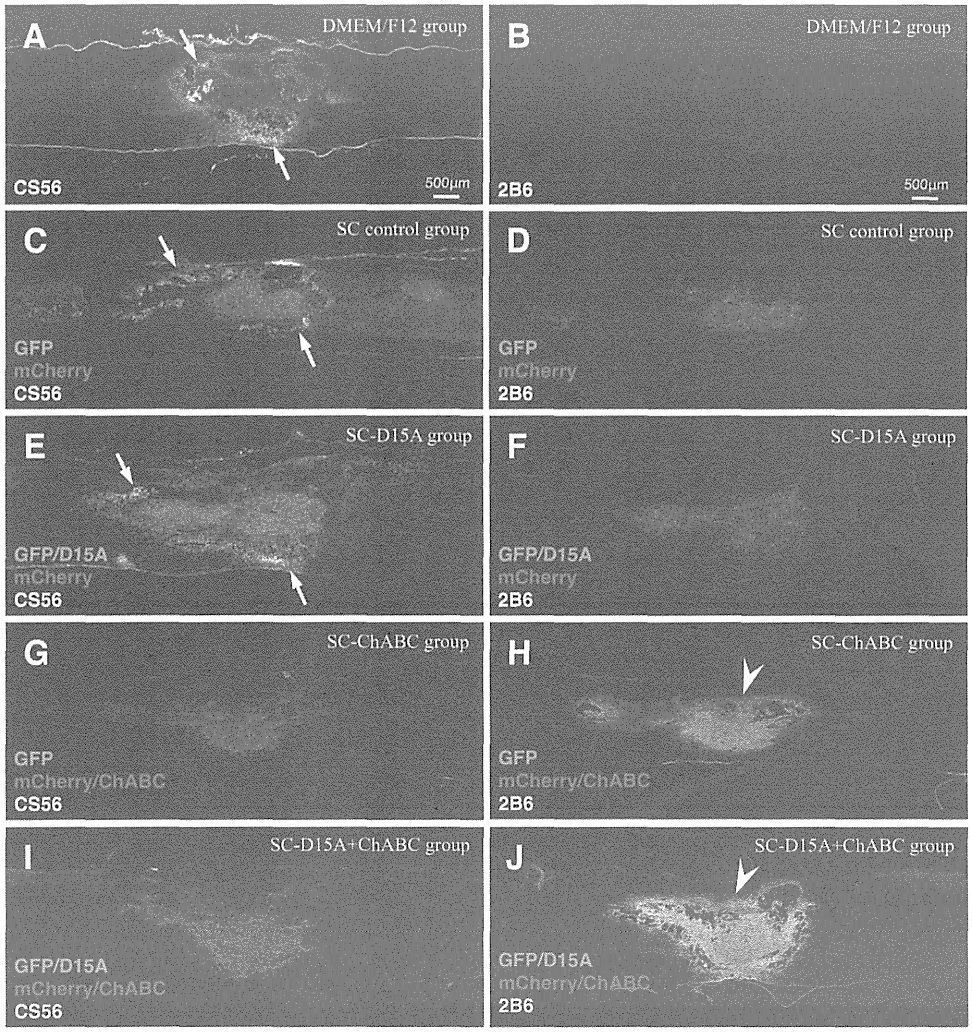

Figure 4. SCs secreting ChABC reduce immunoreactivity for CSPGs in injured spinal cords at 2 weeks after transplantation. After staining for CS56, the groups without ChABC showed higher immunoreactivity around the lesion sites (***A***, ***C***, ***E***, arrows). In contrast, the groups with ChABC did not exhibit such immunoreactivity (***G***, ***I***). After 2B6 staining, higher immunoreactivity was observed both inside and around the transplant in the groups with ChABC (arrowheads in ***H*** and ***J*** vs ***B***, ***D***, ***F***).

means ± SEM. For comparisons among SCs *in vitro*, statistical differences were established using one-way ANOVA followed by a Tukey's *post hoc* test. For immunohistochemical analyses, NT-3 ELISA *in vivo*, DMB assay *in vivo*, and behavioral analyses, significant differences between the treatment groups were assessed using the nonparametric Mann–Whitney *U* test or the parametric Student's *t* test. Differences of $p < 0.05$ were considered to be statistically significant.

Results

D15A-transduced SCs secrete active neurotrophin *in vitro*

The four groups of transduced SCs appeared normal and showed high expression of GFP and mCherry (Fig. 2*A–D*). When DRG were incubated in conditioned medium from D15A/GFP-SC cultures (Fig. 2*F*), neurite outgrowth was robust compared with GFP-SC-conditioned medium (Fig. 2*E*). D10 medium supplemented with BDNF and NT-3 also increased DRG neurite outgrowth (Fig. 2*G*). D15A levels in conditioned medium were determined using an NT-3 ELISA capable of recognizing the NT-3 backbone of D15A. GFP/D15A-SC-conditioned medium contained significantly higher levels of NT-3 (55.0 ± 1.0 ng/ml/24 h, $p < 0.01$) than media from nontransduced SC or GFP-SC controls (which did not contain detectable levels) at 3 d after transduction (Fig. 2*H*).

ChABC-transduced SCs secrete active chondroitinase *in vitro*

After immunostaining for CS56, immunoreactivity in normal spinal cord sections incubated with conditioned medium from ChABC-transduced SC cultures (Fig. 2*J*) and with purified ChABC (Fig. 2*K*) was decreased compared with the sections incubated with PBS (Fig. 2*I*). In contrast, 2B6 immunoreactivity in sections incubated with conditioned medium from ChABC-transduced SCcultures (Fig. 2*M*) and purified ChABC (Fig. 2*N*) was increased compared with sections incubated with PBS (Fig. 2*L*), demonstrating that the enzyme had been active. The DMB assay showed that enzymatic activity in conditioned medium from mCherry/ChABC-SC cultures was significantly higher (3.7 ± 0.6 mU/μl/24 h) than from nontransduced SC cultures (0.2 ± 0.3 mU/μl/24 h, $p < 0.01$) and mCherry-SC cultures (0.4 ± 0.2 mU/μl/24 h, $p < 0.01$) (Fig. 2*O*).

D15A-transduced SCs increase graft volume and SC number

At 12 weeks after transplantation (Fig. 3*A–F*), the graft volumes were significantly larger in the SC-D15A (1.6 ± 0.1 mm^3, $p < 0.01$) and SC-D15A + ChABC groups (2.4 ± 0.2 mm^3, $p < 0.01$) compared with the SC control group (0.7 ± 0.1 mm^3). In addition, the SC-D15A + ChABC group showed a significantly larger